

Role of Pax2 in Apoptosis Resistance and Proinvasive Phenotype of Kaposi's Sarcoma Cells*

Received for publication, June 26, 2003, and in revised form, November 18, 2003
Published, JBC Papers in Press, November 19, 2003, DOI 10.1074/jbc.M306824200

Stefano Buttiglieri, Maria Chiara Deregibus, Stefania Bravo, Paola Cassoni‡, Roberto Chiarle‡, Benedetta Bussolati, and Giovanni Camussi§

From the *Cattedra di Nefrologia, Dipartimento di Medicina Interna and Centro Ricerca Medicina Sperimentale and ‡Dipartimento di Scienze Biomediche e Oncologia, Università di Torino, Torino 10126, Italy*

In this study, we found that Kaposi's sarcoma cells but not human microvascular endothelial cells expressed *PAX2*, a gene coding for a transcription factor involved both in organogenesis and tumorigenesis. Moreover, Pax2 was frequently expressed, on spindle-shaped cells, in Kaposi's sarcoma lesions. We cloned *PAX2* from Kaposi's sarcoma cells and obtained antisense and sense DNA. Transfection of Kaposi's sarcoma cells with antisense DNA, which suppressed Pax2 protein expression, reduced cell growth and survival and enhanced the sensitivity of Kaposi's sarcoma cells to apoptosis induced by serum deprivation or vincristine treatment. In addition, antisense transfection inhibited the cell motility, the invasion of Matrigel, and the spindle shape morphology, which are characteristics of Kaposi's sarcoma cells. Moreover, the $\alpha_v\beta_3$ integrin, known to be involved in tumor invasion, was down-regulated. To evaluate the possible role of Pax2 expression in the endothelial origin of Kaposi's sarcoma cells, human microvascular endothelial cells were transfected with sense DNA. Endothelial cells transfected with sense *PAX2* acquired spindle shape morphology, showed enhanced motility and Matrigel invasion, and displayed an enhanced expression of $\alpha_v\beta_3$ integrin. In conclusion, the expression of Pax2 by Kaposi's sarcoma cells correlated with an enhanced resistance against apoptotic signals and with the proinvasive phenotype. Moreover, *PAX2*-transfected endothelial cells acquired a phenotype resembling that of Kaposi's sarcoma cells, suggesting a role of this embryonic gene in tumorigenesis.

Kaposi's sarcoma (KS)¹ is an angiogenic tumor containing spindle-shaped cells, fibroblasts, inflammatory cells, and vas-

* This work was supported by the Istituto Superiore di Sanità (Targeted Project AIDS), the Associazione Italiana per la Ricerca sul Cancro, the National Research Council, Italian Ministry of University and Research FIRB Project RBNE01HRS5-001, Italian Ministry of Health Ricerca Finalizzata 02, and the special project Oncology Compagnia San Paolo/FIRMS (to G. C.). The costs of publication of this article were defrayed in part by the payment of page charges. This article must therefore be hereby marked "advertisement" in accordance with 18 U.S.C. Section 1734 solely to indicate this fact.

§ To whom correspondence should be addressed: Cattedra di Nefrologia, Dipartimento di Medicina Interna, Ospedale Maggiore S. Giovanni Battista, Corso Dogliotti 14, 10126 Torino, Italy. Tel.: 39-011-6336708; Fax: 39-011-6631184; E-mail: giovanni.camussi@unito.it.

¹ The abbreviations used are: KS, Kaposi's sarcoma; HIV, human immunodeficiency virus; HMEC, human microvascular endothelial cell(s); DMEM, Dulbecco's modified Eagle's medium; FCS, fetal calf serum; Ab, antibody; mAb, monoclonal antibody; ICAM, intracellular adhesion molecule; HUVEC, human microvascular endothelial cell(s); BrdUrd, 5-bromo-2'-deoxyuridine; PBS, phosphate-buffered saline; TUNEL, terminal deoxynucleotidyltransferase-mediated dUTP nick end labeling; FITC, fluorescein isothiocyanate; RT, reverse transcriptase; pNA, p-nitroaniline.

cular endothelial and smooth muscle cells (1–3). KS is frequently associated with conditions of immunodepression such as that occurring in HIV-1 infection and long term post-transplantation therapy (4). The growth and diffusion of KS has been ascribed not only to a dysregulation of cellular proliferation but also to a resistance against apoptotic signals derived from the activation of endogenous or exogenous execution death programs. Several factors may contribute to resistance of apoptosis, including a dysregulation of the cytokine network, which has been implicated in the pathogenesis of KS (5), and the effect of HIV-derived proteins such as Tat (6). Recently, we found that HIV-1 Tat acts as survival factor for KS cells (7) by a mechanism involving a phosphatidylinositol 3-kinase/Akt-dependent pathway (8). In preliminary experiments, we observed by gene array technology that KS cells express in basal conditions several antiapoptotic genes (8).

It has been recently reported that paired box gene 2 (*PAX2*) expression suppresses apoptosis in renal collecting duct cells (9). Pax2 protein is a transcription factor belonging to the evolutionary conserved paired box family involved in organogenesis. Pax2 is required for development of the central nervous system and genitourinary tract. In humans, Pax2 is expressed in induced mesenchyme and in the early epithelial derivatives, and it is rapidly down-regulated in mature kidney (10). The expression of Pax2 was observed in renal cell carcinomas (11) and in mammary tumors (12). A possible role of Pax2 expression in tumor growth has been suggested by using antisense oligonucleotide in renal carcinoma cells (11).

The aim of the present study was to evaluate whether KS cells express Pax2 and whether its expression influences KS cell behavior. For this purpose, KS cells were transfected with the antisense *PAX2* gene to inhibit Pax2 protein expression, and the resistance to apoptosis as well as the growth, the motility and the invasion of Matrigel were evaluated. Moreover, to study the possible role of Pax2 expression in the endothelial origin of Kaposi's sarcoma cells, human microvascular endothelial cells (HMEC) were transfected with sense DNA.

EXPERIMENTAL PROCEDURES

Reagents—Endothelial cell attachment factor, DMEM, and bovine serum albumin fraction V (tested for not more than 1 ng of endotoxin per mg) were purchased from Sigma. Modified MCDB131 medium was obtained from Invitrogen, and fetal calf serum (FCS) was from EuroClone Ltd. (Wetherby, West Yorkshire, UK). Polyclonal rabbit antibody (Ab) against Pax2 was purchased from Covance (Princeton, NJ). Anti- $\alpha_v\beta_3$, - $\alpha_v\beta_5$, and - β_1 mAbs were from Chemicon Int. (Temecula, CA); fluorescein isothiocyanate (FITC)-labeled anti-platelet endothelial cell adhesion molecule mAb was from Euroclone; anti-ICAM-1, anti-CD11 α , and anti-CD11 β mAbs were from BD Biosciences; and anti-E-selectin mAb was from Serotec (Raleigh, NC). Anti- α_v and anti- β_3 monomer mAbs were kindly provided by Guido Tarone (University of Torino, Italy). Vincristine and geneticine were obtained from Sigma.

Detection of Pax2 in KS Lesions by Immunohistochemistry—Surgical sample from eight patients (age range, 49–77 years; sex, 4 male and 4

female patients) with KS were collected. Five were classical cutaneous KS lesions, two were visceral KS (one gastric and one lung primary localization), and one was a lymph node metastasis in a patient with visceral iatrogenic KS. The different cell types were characterized using either morphological criteria or immunohistochemistry with Abs directed toward cell-specific antigens (such as CD34 for spindle cells or factor VIII for vessels) (13). Serial sections from representative paraffin-embedded blocks of human KS lesions were collected onto poly-L-lysine-coated slides and stained for Pax2 antigen. Endogenous peroxidase activity was blocked with 6% H₂O₂ for 5 min at room temperature. Anti-Pax2 Ab was diluted 1:150 in phosphate-buffered saline (PBS) (pH 7.4) and applied to slides overnight at room temperature. Biotin-labeled goat anti-rabbit serum diluted 1:2000 (Sigma) was incubated for 30 min followed by the streptavidin peroxidase LSAB2 method (Dakopatts, Glostrup, Denmark) for the second Ab reaction. The reaction product was developed using 3,3'-diaminobenzidine. Omission of the primary Ab or substitution with an unrelated rabbit serum served as negative control.

Cell Cultures—Four Kaposi's sarcoma cell lines were used: three primary cultures of Kaposi's sarcoma cells (KS cells, KS-C1, and KS-L3) (7, 8) and a spontaneously immortalized cell line (KS-imm) (14). These cell lines were previously characterized (7) in comparison with a well characterized KS cell line (SLK) developed by Herndier *et al.* (39). Cells were cultured with DMEM (Sigma) containing 10% FCS and 2 mM glutamine (Sigma). HMEC were obtained from derma using anti-CD31 Ab coupled to magnetic beads, by magnetic cell sorting using the MACS system (Miltenyi Biotec, Auburn, CA), and immortalized by infection of primary cultures with a replication-defective adeno-5/SV40 virus as previously described (15). Two primary microvascular endothelial cell lines obtained from subcutaneous fat and three umbilical cord vein-derived endothelial cell lines (HUVEC) were prepared as previously described (16). Endothelial cells were characterized as endothelial cells by morphology and positive staining for von Willebrand factor antigen and for CD31, CD105, and the fucosylated receptors for plant lectins (*Ulex europaeus* I and *Bandeira simplicifolia*). Cytoplasmic staining was positive for vimentin and negative for cytokeratin and desmin, as previously described (17). A previously characterized renal carcinoma cell line (K1) was used as positive control for Pax2 expression (18).

Cloning of PAX2 Gene—Total RNA was extracted from KS cells with guanidinium thiocyanate/phenol/chloroform, precipitated with isopropyl alcohol, and washed with 70% ethanol. Two micrograms of RNA were retrotranscribed using oligo(dT) primers and 15 units of reverse transcriptase (RT) enzyme (Eppendorf, Hamburg, Germany). Five microliters of cDNA were amplified with forward and reverse primers (forward, ATGGATATGCACTGCAAAAGCAGA; reverse, CTAGTGGCG-GTCATAGGCAG) covering the initial and terminal part of the coding sequence, respectively (NCBI GenBank™ number GI409138), with *Taq* DNA polymerase (Invitrogen). Amplified DNA was ligated in pTARGET mammalian expression vector (Promega, Madison, WI) under the control of the cytomegalovirus promoter with the T/A cloning system. After sequencing various clones, we identified a clone with Pax2 in correct orientation (S) and a clone with Pax2 in inverse orientation (AS). DNA sequences were compared with the NCBI data base using the BLAST program.

Transfection—Cells were seeded in a 10-cm Petri dish to reach confluence and transfected with 8 µg of DNA and 20 µl of LipofectAMINE 2000 (Invitrogen) in DMEM containing 10% FCS without antibiotics, according to the protocol suggested by the manufacturer. As a control, cells were transfected with the empty plasmid (KS Ctrl). Transfected cells were stably selected by culturing in the presence of 1 mg/ml geneticin. Successful transfection was evaluated by positive immunofluorescence for anti-Pax2 Ab.

Western Blot Analysis—Cells were lysed at 4 °C for 1 h in a lysis buffer (50 mM Tris-HCl, pH 8.3, containing 1% Triton X-100, 10 µM phenylmethylsulfonyl fluoride, 10 µM leupeptin, and 100 units/ml aprotinin) and centrifuged at 15,000 × *g*. The protein contents of the supernatants were measured by the Bradford method. Aliquots containing 10 µg of protein of the cell lysates were subjected to SDS-10% PAGE under reducing conditions and blotted onto nitrocellulose membrane filters. The blots were blocked with 5% nonfat milk in 20 mM Tris-HCl, pH 7.5, 500 mM NaCl plus 0.1% Tween (TBS-T). The membranes were subsequently immunoblotted overnight at 4 °C with the rabbit anti-Pax2 Ab. After extensive washing with TBS-T, the blots were incubated for 1 h at room temperature with peroxidase-conjugated anti-rabbit IgG (Pierce), washed with TBS-T, developed with ECL detection reagents (Amersham Biosciences) for 1 min, and exposed to X-Omat film (Eastman Kodak Co.).

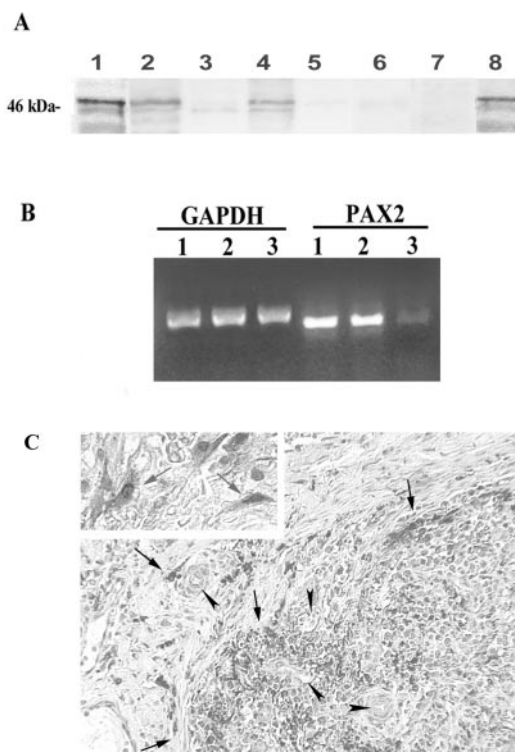


FIG. 1. Pax2 expression in Kaposi's sarcoma cells. **A**, Western blot analysis of Pax2 protein on Kaposi's cell lines, immortalized HMEC, primary microvascular endothelial cells, HUVEC, and K1 renal carcinoma cells used as positive control. Lane 1, KS cells; lane 2, KS-C1; lane 3, KS-L3; lane 4, KS-imm; lane 5, HMEC; lane 6, HUVEC; lane 7, primary microvascular endothelial cells; lane 8, K1 renal carcinoma cells. The results are representative of three independent experiments. **B**, expression of Pax2 mRNA by RT-PCR analysis in KS cells (lane 1), K1 cells (lane 2), and HMEC (lane 3). As control, the expression of glyceraldehyde-3-phosphate dehydrogenase (*GAPDH*) was evaluated. Data are representative of three independent experiments. **C**, a representative micrograph of immunohistochemical staining for Pax2 in a primary cutaneous Kaposi's sarcoma. Several tumor cells infiltrating the subcutaneous tissue (arrows) show nuclear staining for Pax2, whereas vessels are negative (arrowhead) (magnification, ×100). The inset shows the positivity for Pax2 in the characteristic spindle-shaped KS cells (arrows) (magnification, ×400).

RT-PCR—Total RNA was extracted from cells with guanidinium thiocyanate/phenol/chloroform, precipitated with isopropyl alcohol, and washed with 70% ethanol. Two micrograms of RNA were retrotranscribed using oligo(dT) primers and 15 units of RT enzyme (Eppendorf). Two microliters of cDNA were amplified with forward (ATGGATATGCACTGCAAAAGCAGA) and reverse (CGTGCTGGGACAATGGTGTG) primers, with *Taq* DNA polymerase (Invitrogen). Reactions were performed for 30 cycles at a melting temperature of 52 °C and analyzed with a BrEtOH 1.5% agarose gel.

Cell Proliferation Assay—Cells were seeded at 8,000 cells/well into 96-well plates in DMEM containing 10% FCS and allowed to adhere. DNA synthesis was detected as incorporation of 5-bromo-2'-deoxyuridine (BrdUrd) into the cellular DNA using an enzyme-linked immunosorbent assay kit (Roche Applied Science), following the manufacturer's instructions. Briefly, after washing, cells were added with 10 µM BrdUrd and incubated in DMEM without FCS or in DMEM plus 10% FCS for 18 h. Cells were then fixed with 0.5 M ethanol/HCl and incubated with nuclease to digest the DNA. BrdUrd incorporated into the DNA was detected using an anti-BrdUrd peroxidase-conjugated mAb and visualized with a soluble chromogenic substrate. Optical density was measured with an enzyme-linked immunosorbent assay reader at 405 nm.

Cell Cycle Analysis—Cells were seeded on 6-well plates in the presence or in absence of serum and analyzed after a 24-h incubation at 37 °C. Cells were trypsinized, washed in PBS, and incubated for 1 h at 4 °C in 1 ml of hypotonic solution containing 50 µg/ml propidium iodide, 0.1% sodium citrate, 0.1% Triton X-100, and 20 µg/ml DNase-free RNase A. Cells were analyzed with flow cytometry in linear mode. Results were expressed as percentages of elements detected in the

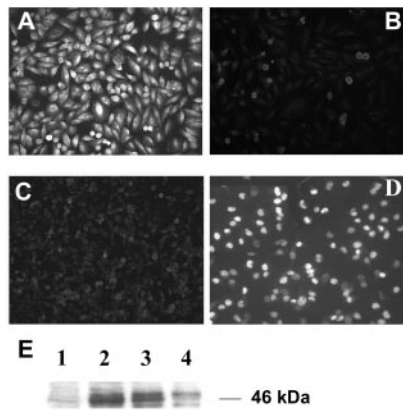


FIG. 2. Transfection of KS cells and HMEC with antisense and sense vectors. A–D, immunofluorescence staining of Pax2 was evaluated in KS-Ctrl (A), KS-AS (B), HMEC-Ctrl (C), and HMEC-S (D). Transfection of KS cells with *PAX2* antisense vector markedly reduced the immunofluorescence staining for Pax2 with respect to KS-Ctrl transfected with the empty vector. HMEC that showed minimal staining of Pax2 protein (C) were conversely positive after transfection with the vector containing sense *PAX2* (D). Micrographs are representative of three individual experiments. Magnification was $\times 400$. E, representative Western blot analysis showing Pax2 protein expression in HMEC-Ctrl (lane 1), HMEC-S (lane 2), KS-Ctrl (lane 3), and KS-AS cells (lane 4). Data are representative of three independent experiments.

different phases of the cell cycle, namely sub- G_1 peak (apoptosis), G_0/G_1 (no DNA synthesis), S (active DNA synthesis), G_2 (premitosis), and M (mitosis).

Assessment of Apoptosis—Apoptosis was evaluated using the TUNEL assay analysis (ApopTag Oncor, Gaithersburg, MD). After serum withdrawal and/or treatment with 0.25 $\mu\text{g}/\text{ml}$ vincristine for 24 h, cells were suspended in PBS and fixed in 1% paraformaldehyde in PBS, pH 7.4, for 15 min at 4 °C and then fixed in precooled ethanol/acetic acid (2:1) for 5 min at –20 °C. Cells were treated with terminal deoxynucleotidyltransferase enzyme and incubated in a humidified chamber at 37 °C for 1 h and then with FITC-conjugated anti-digoxigenin for 30 min at room temperature. After washings, samples were mounted in medium containing 1 $\mu\text{g}/\text{ml}$ propidium iodide, and the cells were analyzed by immunofluorescence. Results are expressed as a percentage of green fluorescence-emitting cells (apoptotic cells) versus red fluorescence-emitting cells (total cells).

Detection of Caspase-3 and -9 Activity—Activation of caspase-3 and -9 was assessed by a colorimetric assay (Chemicon International) based on spectrophotometric detection of the chromophore *p*-nitroanilide (*p*NA) after cleavage from the labeled substrate DEVD-*p*NA, which is recognized by caspase-3, and LEHD-*p*NA, which is recognized by caspase-9. Lysates of treated or untreated cells were diluted 1:1 with 2 \times reaction buffer (10 mM Tris (pH 7.4), 1 mM dithiothreitol, 2 mM EDTA, 1 mM phenylmethylsulfonyl fluoride, 0.1% (3-(3-cholamido-propyl)dimethylammonio)-1-propanesulfonate, pepstatin (10 $\mu\text{g}/\text{ml}$), and leupeptin (10 $\mu\text{g}/\text{ml}$)). DEVD-*p*NA or LEHD-*p*NA was added at a final concentration of 50 μM , and the reaction was incubated for 1 h at 37 °C. The absorption values were measured at 405 nm in an enzyme-linked immunosorbent assay reader.

In Vitro Cell Migration—A total of 1×10^5 cells/well were plated in DMEM containing 10% FCS. Cell migration was studied over a 4-h period under a Nikon Diaphot inverted microscope with a $\times 20$ phase-contrast objective in an attached, hermetically sealed Plexiglas Nikon NP-2 incubator at 37 °C. Cell migration was recorded using a JVC-1CCD video camera. Image analysis was performed with a MicroImage analysis system (Cast Imaging srl, Venice, Italy) and an IBM-compatible system equipped with a video card (Targa 2000; Truevision, Santa Clara, CA). Image analysis was performed by digital saving of images at 15-min intervals. Migration tracks were generated by marking the positions of the nuclei of individual cells on each image. The net migratory speed (velocity straight line) was calculated by the MicroImage software based on the straight line distance between the starting and ending points divided by the time of observation (17). Migration of at least 30 cells was analyzed for each experimental condition. Values are given as means \pm S.D.

Matrigel Invasion Assay—The assay for matrix invasion was performed in Transwell chambers (Costar, Cambridge, MA), by seeding 10^5

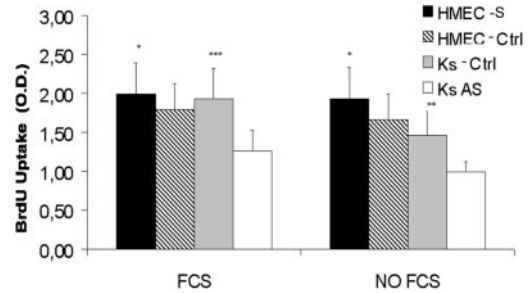


FIG. 3. Effect of transfection of KS cells and HMEC with the *PAX2* antisense or sense vectors on proliferation. Cells were incubated overnight with BrdUrd, fixed, and stained with anti-BrdUrd antibody horseradish peroxidase-linked in a colorimetric reaction. The figure shows a significant reduction in proliferation in cells transfected with *PAX2* antisense. Proliferation was, conversely, significantly enhanced in *PAX2*-transfected HMEC. Results are expressed as mean \pm S.D. of eight experiments. Analysis of variance with Dunnett's multi-comparison test was performed versus control. *, $p < 0.005$; ***, $p < 0.001$.

cells on the upper side porous polycarbonate membrane of 8- μm pore size coated with 12.5 μg of Matrigel (Becton Dickinson, Bedford, MA) as previously described (19). Cells migrated through the membrane of the lower side of the filter were counted after 24- or 72-h incubation by a computer-assisted analysis system (Cast Imaging).

Immunofluorescence and Cytofluorimetric Analysis—Cultured cells were fixed for 10 min in a 4:1 mixture of acetone/chloroform, air-dried, and kept at –80 °C until use. The cells were then washed twice in PBS, blocked for 30 min with 5% bovine serum albumin in PBS, and then incubated with the primary rabbit anti-Pax2 Ab diluted in PBS-bovine serum albumin (1:100) and with the secondary FITC-conjugated goat anti-rabbit IgG Ab (Dako, Copenhagen, Denmark) and visualized on a Leica microscope with fluorescence optics.

For cytofluorimetric analysis, cells were detached from plates with nonenzymatic cell dissociation solution, washed in PBS containing 2% heat-inactivated human serum, and incubated for another 15 min with whole heat-inactivated human serum to block the remaining nonspecific sites. Cells were then incubated for 30 min at 4 °C with the appropriate Ab or with the irrelevant control in PBS containing 2% heat-inactivated human serum. Where a second step reagent was needed, cells were stained by the addition of FITC-conjugated goat anti-mouse IgG and incubated for a further 30 min at 4 °C. Cells were analyzed on a fluorescence-activated cell sorter (Becton Dickinson, Mountain View, CA). 10,000 cells were analyzed in each experimental point.

Scanning Electron Microscopy—Cells were fixed in Karnovsky's fixative for 1 h, dehydrated in alcohol, dried, and coated with gold by sputter coating and examined in a scanning electron microscope (Jeol JSM T300) operating at 25 kV.

RESULTS

The expression of Pax2 protein was evaluated by Western blot analysis on four Kaposi's cell lines, on immortalized HMEC, on two primary microvascular endothelial cell lines, on three HUVEC lines, and on K1 renal carcinoma cells used as a positive control. As shown in Fig. 1A, KS cells, KS-imm, and KS-C1 as well as K1 renal carcinoma cells strongly expressed Pax2 protein. The expression of Pax2 protein by KS-L3 was minimal. In contrast, all of the different endothelial cell lines were negative. The expression of Pax2 mRNA from KS cells was confirmed by RT-PCR (Fig. 1B). To evaluate the *in vivo* expression of Pax2 in Kaposi's sarcoma, immunohistochemical analysis was performed on five classical cutaneous and two visceral KS lesions and on lymph node metastases. The results obtained indicate that three cutaneous and two noncutaneous lesions (the gastric KS localization and the lymph node metastases) were positive for Pax2 expression on fusate spindle-shaped lesional cells (Fig. 1C), whereas vessels were negative.

To study the possible relevance of Pax2 expression, the *PAX2* gene was cloned from KS cells. Amplified DNA was ligated in

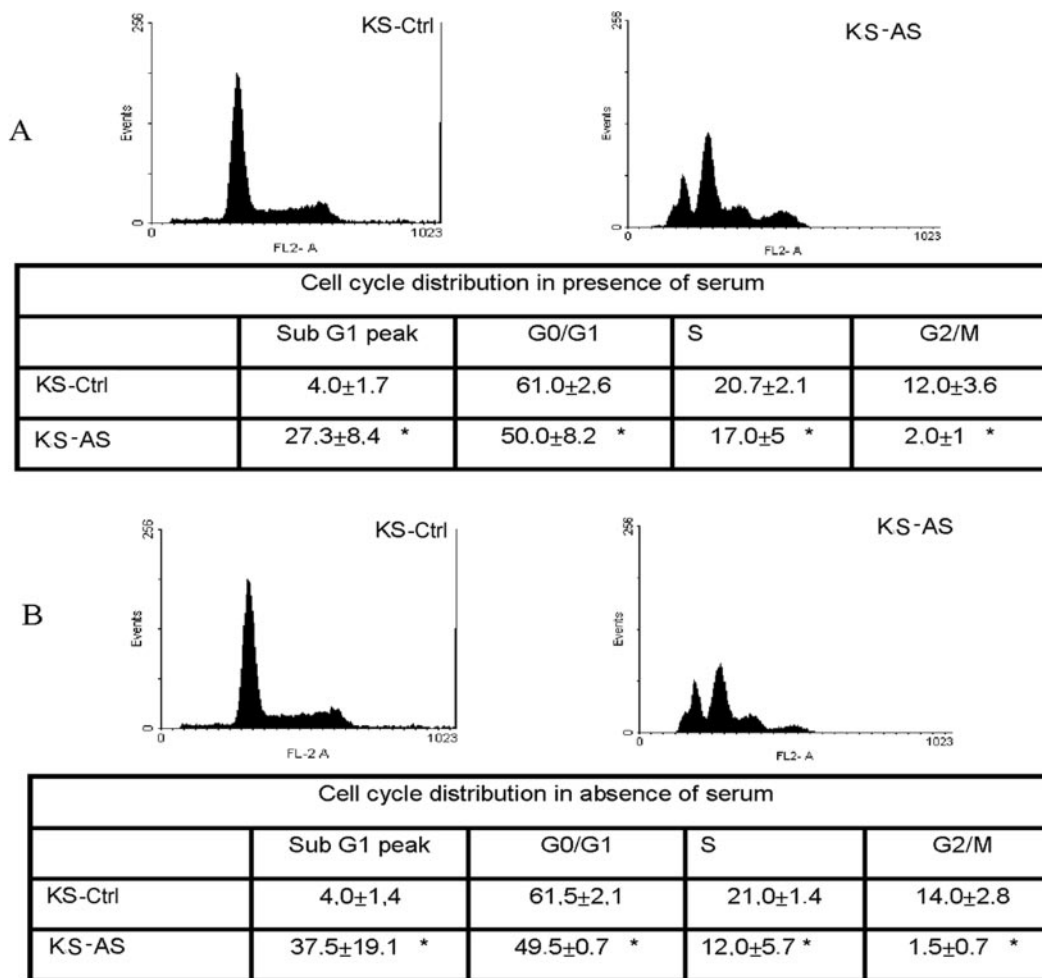


FIG. 4. Cell cycle analysis of KS-AS cells transfected with PAX2 antisense and of KS-Ctrl cells transfected with the empty vector. A shows a representative experiment and the summary table of cell cycle distribution in cells cultured in the presence of FCS; B shows a representative experiment and the summary table of cell cycle distribution in cells cultured in the absence of serum. Data represent mean \pm S.D. of five experiments. Analysis of variance with Dunnett's multicomparison test was performed *versus* controls. *, $p < 0.005$.

pTARGET mammalian expression vector under the control of cytomegalovirus promoter with the T/A cloning system. After sequencing various clones, we identified a clone with PAX2 in correct orientation (S) and a clone with PAX2 in inverse orientation (AS). KS cells were stably transfected with PAX2 in inverse orientation (KS-AS), and the Pax2 protein expression was evaluated. As shown in Fig. 2, the immunofluorescence staining of Pax2 was markedly reduced in KS-AS (Fig. 2B) with respect to KS-Ctrl transfected with the empty vector (Fig. 2A). The reduced expression of Pax2 protein in KS-AS cells was confirmed by Western blot analysis (Fig. 2E). HMEC, which express a minimal amount of Pax2 protein (Fig. 2C), were conversely transfected with the vector containing sense DNA (HMEC-S) in order to obtain expression of Pax2 (Fig. 2D).

As shown in Fig. 3, the growth of KS-AS cells was significantly reduced both in the presence or in the absence of FCS with respect to KS-Ctrl. Transfection of HMEC with sense PAX2 significantly enhanced cell BrdUrd uptake.

Cell cycle analysis showed a significant reduction of G₂/M and S peaks in KS-AS with respect to KS-Ctrl (Fig. 4). In addition, a marked increase in sub-G₁ peak was observed both in the presence or absence of FCS, suggesting an enhanced apoptosis in cells transfected with PAX2 antisense.

An enhanced sensitivity to apoptosis of KS-AS cells with respect to KS-Ctrl was also detected by a TUNEL assay (Fig. 5A). This was already detectable in the presence of FCS and

markedly enhanced after serum starvation and vincristine treatment. The antiapoptotic effect of Pax2 was confirmed by the observation that HMEC-S were significantly more resistant to apoptosis induced both by serum deprivation and vincristine with respect to HMEC-Ctrl. The increased sensitivity of KS-AS to apoptosis was also indicated by the enhanced activation of caspase-9 and -3 after serum deprivation and vincristine treatment (Fig. 5, B and C).

The basal motility of KS cells detected by time lapse cinematography was significantly decreased in KS-AS with respect to KS-Ctrl (Fig. 6, A-C). Conversely, transfection of HMEC with PAX2 sense DNA significantly enhanced cell motility with respect to HMEC-Ctrl (Fig. 6, A, D, and E).

The *in vitro* invasive property in Matrigel and the spindle shape morphology are considered characteristic features of KS lesional cells (20-24). We therefore evaluated the effect of Pax2 expression on these properties. As shown in Fig. 7, invasiveness of Matrigel by KS-AS was significantly reduced with respect to KS-Ctrl, whereas invasiveness of Matrigel by HMEC-S was significantly enhanced with respect to HMEC-Ctrl. Moreover, KS-AS lost the characteristic spindle shape morphology observed in KS-Ctrl (Fig. 8, A-D). In analogy to this result, HMEC-S tended to develop a spindle shape resembling that of KS cells (Fig. 8, E-H).

To investigate the potential mechanism by which Pax2 may regulate the invasive phenotype, we studied the effect of trans-

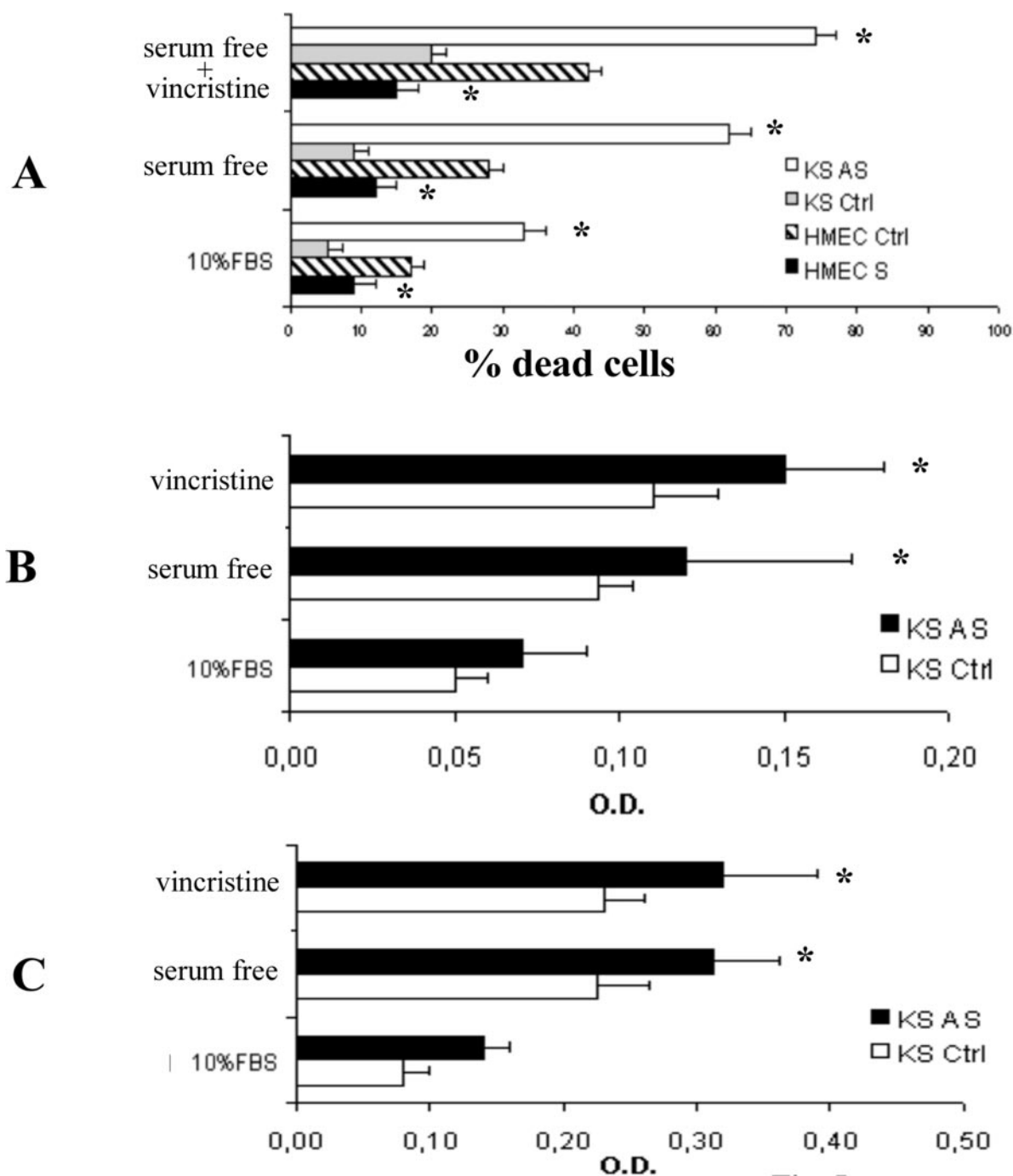


FIG. 5. Effect of transfection of KS cells and HMEC with the PAX2 antisense or sense vectors on apoptosis. A, apoptosis was evaluated by the TUNEL assay as a percentage of apoptotic cells after 24-h serum withdrawal or treatment with 0.25 μ g/ml vincristine. B shows the activation of caspase-3, and C shows the activation of caspase-9 assessed by a colorimetric assay (see "Experimental Procedures") in KS-AS and KS-Ctrl after 24-h serum withdrawal or treatment with 0.25 μ g/ml vincristine. Data are expressed as mean \pm S.D. of three independent experiments. Analysis of variance with Dunnett's multicomparison test was performed versus controls. *, $p < 0.005$.

fection of KS cells with PAX2 antisense and of HMEC with PAX2 sense on several adhesion molecules. As shown in Fig. 9, the $\alpha_v\beta_3$ dimer was significantly down-regulated in KS-AS and up-regulated in HMEC-S in comparison with the respective controls. The observed variations of the $\alpha_v\beta_3$ dimer were due to changes in the expression of the β_3 monomer (KS-AS, $12.2 \pm 3.5\%$; KS-Ctrl, $82.2 \pm 4.7\%$; HMEC-S, $78 \pm 7.2\%$; HMEC-Ctrl, $19.4 \pm 3.4\%$), whereas the expression of the α_v monomer was unchanged (KS-AS, $95.7 \pm 1.8\%$; KS-Ctrl, $98.3 \pm 2.3\%$; HMEC-S, $75.8 \pm 5.3\%$; HMEC-Ctrl, $72.1 \pm 7.0\%$). No significant changes in $\alpha_v\beta_5$, β_1 , CD11 α and CD11 β , platelet endothe-

lial cell adhesion molecule, ICAM-1, and E-selectin were observed (data not shown).

DISCUSSION

In the present study, we demonstrated that KS cells express Pax2 and that its expression contributes to resistance to apoptosis and the proinvasive phenotype of KS cells.

Aside from dysregulation of cellular proliferation, the resistance to apoptotic signals has been implicated in the pathogenesis of KS. Indeed, KS cells, despite the expression of Fas on their surface, were shown to be resistant to Fas-mediated apo-

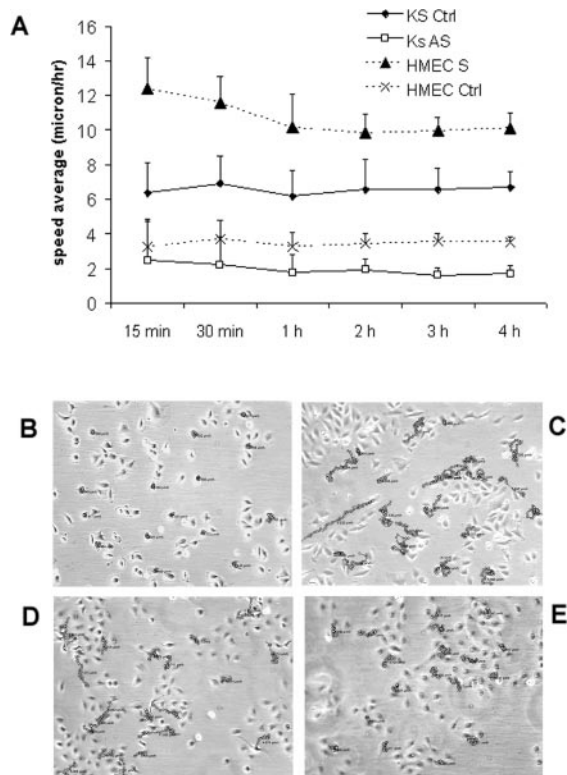


FIG. 6. Effect of transfection of KS cells and HMEC with the PAX2 antisense or sense vectors on *in vitro* cell migration. Motility was performed by digital saving at 15-min intervals over a 4-h period of cells incubated at 37 °C with 10% FCS. A shows means \pm S.D. of three independent experiments. B–E show representative micrographs of the time lapse analysis of KS-AS (B), KS-Ctrl (C), HMEC-S (D), and HMEC-Ctrl (E). Migration tracks (magnification, $\times 120$) were generated by marking the position of the nucleus of individual cells in each image (see “Experimental Procedures”).

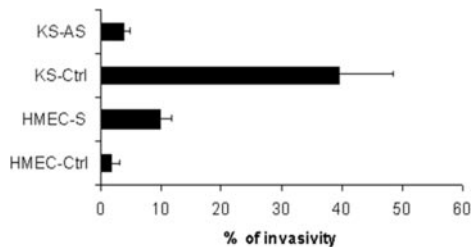


FIG. 7. Effect of transfection of KS cells and HMEC with the PAX2 antisense or sense vectors on the *in vitro* Matrigel invasion assay. The matrix invasion assay was performed by seeding 10^5 cells on the upper side of porous polycarbonate membrane of 8- μ m pore size coated with 12.5 μ g of Matrigel. Cells migrated through the membrane at the lower side of the filter were counted in the lower side of the transwells after incubation of KS-Ctrl and KS-AS for 24 h and of HMEC-Ctrl and HMEC-S for 72 h. Results are expressed as a percentage of migrated cells with respect to total cells seeded. Data are the mean \pm S.D. of three different experiments.

ptosis (25). In addition, KS cells derived from AIDS patients were reported to be often resistant to chemotherapy drugs (26). We recently demonstrated that HIV-1 Tat has an antiapoptotic effect on vincristine-treated KS cells (8). Gene expression analysis by Gene array technology demonstrated that KS cells expressed several antiapoptotic genes, including *Akt-1* and *Akt-2*, *Bcl2*, *Bcl-xL*, *MCL-1*, and insulin-like growth factor 1 (8). *PAX2*, a gene coding for a transcription factor belonging to the evolutionary conserved paired box family involved in organogenesis (27), has been recently shown to protect renal collecting duct cells from apoptosis. Moreover, it has been shown that *PAX2* is frequently expressed in primary human cancers, sug-

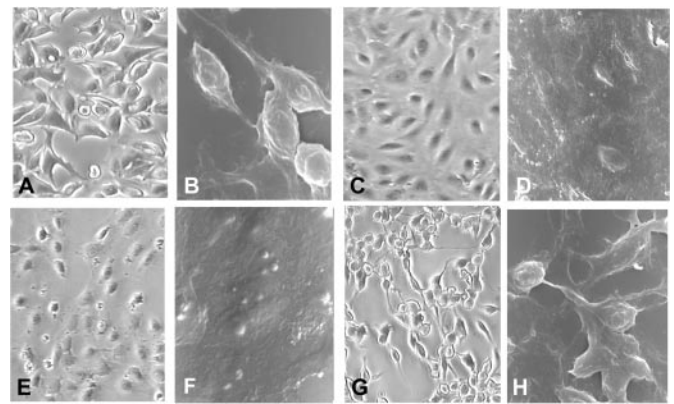


FIG. 8. Micrographs representative of the morphological changes induced by transfection of KS cells and HMEC with the PAX2 antisense or sense vectors. KS-Ctrl showed characteristics spindle cell morphology by phase-contrast (A) and scanning electron microscopy (B). KS-AS showed the loss of spindle shape morphology after transfection with *PAX2* antisense by phase-contrast (C) and scanning electron microscopy (D). HMEC-Ctrl showed the characteristic cobblestone-like appearance by phase-contrast (E) and a very flattened appearance with nuclei and nucleoli protruding from the even surface by scanning electron microscopy (F). After transfection with *PAX2* sense vector, HMEC-S tended to lose contact with neighbor cells and developed a spindle shape morphology (G and H). A, C, E, and G, magnification was $\times 250$; B, D, F, and H, magnification was $\times 1000$. Three different experiments were performed with similar results.

gesting its possible involvement in the cancer pathogenesis (10, 11, 28). In the present study, we found that several Kaposi's sarcoma cell lines markedly expressed both Pax2 mRNA and Pax2 protein. The immunohistochemical analysis of classical cutaneous and visceral and lymphatic KS lesions suggests that Pax2 is frequently expressed in KS lesional cells *in vivo*. However, the expression of Pax2 was not detected in all tumors, and in positive tumors only a variable fraction of tumor cells expressed this protein. This is consistent with immunohistochemical studies on other primary tumors, suggesting that *PAX2* gene function is required only at certain stages of tumor cell development (28).

These results prompted us to evaluate whether Pax2 expression plays a role in the KS tumorigenesis. A previous study demonstrated that when renal carcinoma cells expressing high levels of Pax2 were treated with antisense Pax2 oligonucleotides, *in vitro*, cell number was dramatically reduced (11). In the present study, *PAX2* was cloned from KS cells, and antisense and sense DNA were obtained. Transfection of KS cells with antisense DNA inhibited incorporation of BrdUrd, suggesting a reduced growth. The analysis of the cell cycle evidenced a significant difference in the S or G₂/M phases between KS-AS and control cells transfected with the empty vector. Moreover, cells in the hypodiploid phase (sub-G₁ peak) were significantly increased in KS-AS, suggesting that transfection with *PAX2* antisense had a major effect on apoptosis. It has been recently shown that high levels of Pax2 protein were necessary for survival of renal collecting duct cells and optimal branching morphogenesis during renal development. Expression of Pax2 in renal cells was shown to protect these cells against apoptotic death induced by caspase 2 (9). In the present study, we observed by TUNEL assay that transfection with *PAX2* antisense DNA significantly increased the number of apoptotic KS cells in basal conditions and enhanced the sensitivity of KS cells to apoptosis induced by serum deprivation or vincristine treatment. The observation that transfection of HMEC with sense *PAX2* DNA conferred resistance to apoptosis and to a minor extent stimulated proliferation confirms that Pax2 primary function is antiapoptotic. An association has

A

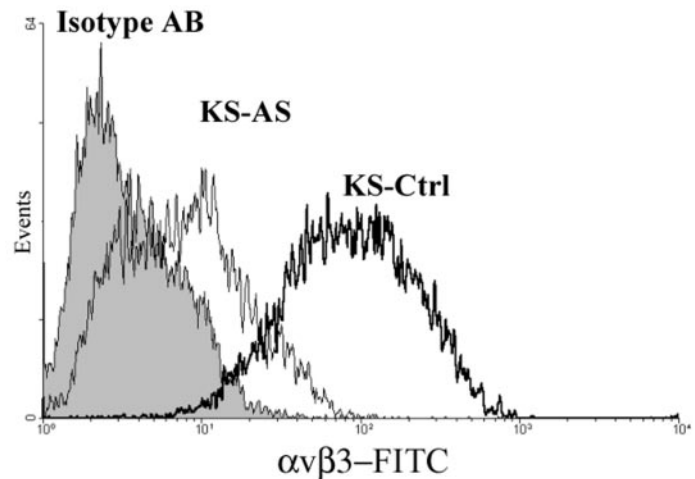
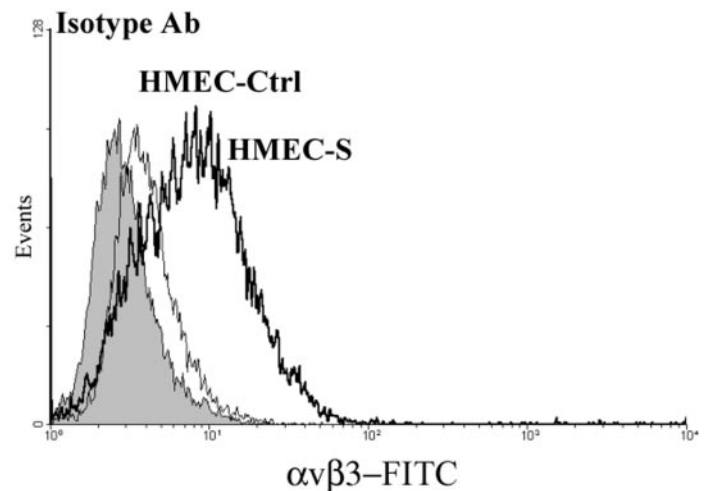


FIG. 9. Effect of transfection of KS cells with PAX2 antisense and of HMEC with PAX2 sense on adhesion molecules. A shows the $\alpha_v\beta_3$ dimer expression in KS-Ctrl (dark line; $82 \pm 3\%$ of cells) and in KS-AS (gray line; $14 \pm 2\%$ of cells). B shows the $\alpha_v\beta_3$ dimer expression in HMEC-Ctrl (gray line; $12 \pm 3\%$ of cells) and in HMEC-S (dark line; $63 \pm 5\%$ of cells). $\alpha_v\beta_3$ dimer was significantly down-regulated in KS-AS and up-regulated in HMEC-S in comparison with the respective controls. The filled area shows the isotype controls. The figure is representative of three different experiments. Kolmogorov-Smirnov statistical analysis between transfected and control cells was performed in each individual experiment.

B



been reported between apoptosis and other members of the paired box gene families (9). Pax3 mutant mice exhibited increased apoptosis of somatic mesoderm (29). Pax2, Pax5, and Pax8 all inhibit transcription of p53, a pivotal molecule regulating the final common apoptotic pathway (30, 31). In addition, Pax6 mutation has been shown to correlate with an excessive apoptosis of photoreceptor precursor (32).

The possible relevance of Pax2 expression to pathogenesis of KS is also supported by the inhibitory effect of antisense transfection on cell motility, invasion of Matrigel, and spindle shape morphology, which are characteristics of KS cells. Although the exact origin of KS spindle cells remains unclear, it appears that these cells may have a mesenchymal origin. It has been suggested that KS cells may derive from lymphatic endothelial cells or vascular cell precursors that were infected by HHV-8. Indeed, *in vitro* experiments demonstrated that HHV-8 is able to infect endothelial cells, inducing a spindle cell morphology and increasing proliferative life span (33, 34). In the present study, transfection of HMEC with sense PAX2 induced spindle shape morphology and enhanced motility and Matrigel invasive properties, suggesting the involvement of PAX2 in the possible origin of KS cells from endothelium. A potential mechanism by which Pax2 may regulate the invasive phenotype is the modulation of integrin expression. Indeed, we observed that the $\alpha_v\beta_3$ dimer was significantly down-regulated in KS

transfected with PAX2 antisense and up-regulated in HMEC transfected with PAX2 sense. Independent of its role in tumor angiogenesis, integrin $\alpha_v\beta_3$ has been implicated in the pathogenesis of various cancers. This is particularly apparent for KS, where $\alpha_v\beta_3$ is highly expressed *in vitro* and *in vivo* (35–37).

In humans, the oncogenic potential of Pax2 remains to be determined. In mice, it has been shown that the induction of tumor formation was dependent on the type of paired domain but did not require the presence of homeodomain. It has been suggested that the oncogenic potential of Pax proteins is dependent on the DNA-binding function of the paired motif. Therefore, not only the Pax3 and Pax6 proteins containing intact homeodomain, but also Pax2 and Pax8 containing residual homeodomain and Pax1, completely lacking a homeodomain, were able to induce transformation of cell culture and tumor formation in mice (38).

In the present study, the expression of Pax2 by KS cells correlated with enhanced resistance against apoptotic signals derived from activation of endogenous execution programs and exogenous stimuli and with the proinvasive phenotypes of KS cells.

Altogether, these results suggest that Pax gene products are not only involved in controlling embryogenesis, but, if deregulated, they can also induce tumorigenesis.

REFERENCES

1. Ensoli, B., Barillari, G., Salahuddin, S. Z., Gallo, R. C., and Wong-Staal, F. (1990) *Nature* **345**, 84–86
2. Gallo, R. C. (1998) *Science* **282**, 1837–1839
3. Rabkin, C. S., Janz, S., Lash, A., Coleman, A. E., Musaba, E., Lotta, L., Biggar, R. J., and Zhuang, Z. (1997) *N. Engl. J. Med.* **336**, 988–993
4. Mitsuyasu, R. T. (2000) *Curr. Opin. Oncol.* **12**, 174–180
5. McCloskey, T. W., Ott, M., Tribble, E., Khan, S. A., Teichberg, S., Paul, M. O., Pahwa, S., Verdin, E., and Chirmule, N. (1997) *J. Immunol.* **158**, 1014–1019
6. Westendorp, M. O., Frank, R., Ochsenbauer, C., Stricker, K., Dhein, J., Walczak, H., Debatin, K. M., and Krammer, P. H. (1995) *Nature* **375**, 497–500
7. Cantaluppi, V., Biancone, L., Boccellino, M., Doublier, S., Benelli, R., Carlone, S., Albini A., and Camussi, G. (2001) *AIDS* **10**, 965–976
8. Deregibus, M. C., Cantaluppi, V., Doublier, S., Brizzi, M. F., Deambrosis, I., Albini, A., and Camussi, G. (2002) *J. Biol. Chem.* **277**, 25195–25202
9. Torban, E., Eccles, M. R., Favor, J., and Goodyer P. R. (2000) *Am. J. Pathol.* **157**, 833–842
10. Dressler, G. R., and Douglass, E. C. (1992) *Proc. Natl. Acad. Sci. U. S. A.* **89**, 1179–1183
11. Gnarra, J. R., and Dressler, G. R. (1995) *Cancer Res.* **55**, 4092–4098
12. Silberstein, G. B., Dressler, G. R., and Van Horn, K. (2002) *Oncogene* **21**, 1009–1016
13. Cassoni, P., Sapino, A., Deaglio, S., Bussolati, B., Volante, M., Munaron, L., Albini, A., Torrisi, A., and Bussolati, G. (2002) *Cancer Res.* **15**, 2406–2413
14. Albini, A., Paglieri, I., and Orengo, G. (1997) *AIDS* **11**, 713–721
15. Conaldi, P. G., Serra, C., Mossa, A., Falcone, V., Basolo, F., Camussi, G., Dolei, A., and Toniolo, A. (1997) *J. Infect. Dis.* **175**, 693–696
16. Bussolati, B., Deambrosis, I., Russo, S., Deregibus, M. C., and Camussi, G. (2003) *FASEB J.* **17**, 1159–1161
17. Deregibus, M. C., Buttiglieri, S., Russo, S., Bussolati, B., and Camussi, G. (2003) *J. Biol. Chem.* **278**, 18008–18014
18. Bussolati, B., Russo, S., Deambrosis, I., Cantaluppi, V., Volpe, A., Ferrando, U., and Camussi, G. (2002) *Int. J. Cancer.* **100**, 654–661
19. Albini, A., Iwamoto, Y., Kleinman, H. K., Martin, G. R., Aarson, S. A., Kozlowski, J. M., and McEwan, R. N. (1987) *Cancer Res.* **47**, 3239–3245
20. Becksted, J. H., Woods, G. S., and Fletcher, V. (1985) *Am. J. Pathol.* **119**, 294–300
21. Corbeil, J., Evans, L. A., Vasak, E., Cooper, D. A., and Penney, R. (1991) *J. Immunol.* **146**, 2972–2976
22. Jussila, L., Valtola, R., Partanen, T. A., Salven, P., Heikkila, P., Matikainen, M. T., Renkonen, R., Kalpainen, A., Detmar, M., Tschachler, E., Alitalo, R., and Alitalo, K. (1998) *Cancer Res.* **58**, 1599–1604
23. Salahuddin, S. Z., Nakamura, S., Biberfeld, P., Kaplan, M. H., Markham, P. D., Arsson, L., and Gallo, R. C. (1998) *Science* **242**, 430–433
24. Scully, P. A., Steinman, H. K., Kennedy, C., Trueblood, K., Frisman, D. M., and Voland, J. R. (1988) *Am. J. Pathol.* **130**, 244–251
25. Mori, S., Murakami-Mori, K., Jewett, A., Nakamura, S., and Bonavida, B. (1996) *Cancer Res.* **56**, 1874–1879
26. Lee, F. C., and Mitsuyasu, R. T. (1996) *Hematol. Oncol. Clin. North Am.* **10**, 1051
27. Dahl, E., Koseki, H., and Baling, R. (1997) *BioEssays* **19**, 755–765
28. Muratovska, A., Zhou C., He, S., Goodyer, P., and Eccles, M. R. (2003) *Oncogene* **11**, 6045–6053
29. Borycku, A. G., Li, J., Emerson, C. P., Jr., and Epstein, J. A. (1999) *Development* **126**, 1665–1674
30. Stuart, E. T., Haffner, R., Oren, M., and Gruss, P. (1995) *EMBO J.* **14**, 5638–5645
31. Levine, A. J. (1997) *Cell* **8**, 323–331
32. Halder, G., Callaerts, P., Flister, S., Walldorf, U., Kloter, U., and Gering, W. J. (1998) *Development* **125**, 2181–2191
33. Flore, O., Rafii, S., Ely, S., O'Leary, J. J., Hyjek, E. M., and Cesarman, E. (1998) *Nature* **394**, 588–592
34. Moses, A. V., Fish, K. N., Ruhl, R., Smith, P. P., Strussenberg, J. G., Zhu, L., Chandran, B., and Nelson, J. A. (1999) *J. Virol.* **73**, 6892–6902
35. Ensoli, B., Gendelman, R., Markham, P., Fiorelli, V., Colombini, S., Raffeld, M., Cafaro, A., Chang, H. K., Brady, J. N., and Gallo, R. C. (1994) *Nature* **371**, 674–680
36. Uccini, S., Ruco, L. P., Monardo, F., Stoppacciaro, A., Dejana, E., La Parola, I. L., Cerimele, D., and Baroni, C. D. (1994) *J. Pathol.* **173**, 23–31
37. Kaaya, E. E., Castanos-Velez, E., Amir, H., Lema, L., Luande, J., Kitinya, J., Patarroyo, M., and Biberfeld, P. (1996) *Histopathology* **29**, 337–346
38. Maulbecker, C. C., and Gruss, P. (1993) *EMBO J.* **12**, 2361–2367
39. Herndier, B., Werner, A., and Arnstein, P. (1994) *AIDS* **8**, 575–581

Role of Pax2 in Apoptosis Resistance and Proinvasive Phenotype of Kaposi's Sarcoma Cells

Stefano Buttiglieri, Maria Chiara Deregibus, Stefania Bravo, Paola Cassoni, Roberto Chiarle, Benedetta Bussolati and Giovanni Camussi

J. Biol. Chem. 2004, 279:4136-4143.

doi: 10.1074/jbc.M306824200 originally published online November 19, 2003

Access the most updated version of this article at doi: [10.1074/jbc.M306824200](https://doi.org/10.1074/jbc.M306824200)

Alerts:

- [When this article is cited](#)
- [When a correction for this article is posted](#)

[Click here](#) to choose from all of JBC's e-mail alerts

This article cites 39 references, 13 of which can be accessed free at <http://www.jbc.org/content/279/6/4136.full.html#ref-list-1>